

ARTICLE

<https://doi.org/10.1038/s41467-019-11676-x>

OPEN

Thermodynamic efficiency in dissipative chemistry

Emanuele Penocchio ¹, Riccardo Rao ^{1,2} & Massimiliano Esposito¹

Chemical processes in closed systems inevitably relax to equilibrium. Living systems avoid this fate and give rise to a much richer diversity of phenomena by operating under nonequilibrium conditions. Recent experiments in dissipative self-assembly also demonstrated that by opening reaction vessels and steering certain concentrations, an ocean of opportunities for artificial synthesis and energy storage emerges. To navigate it, thermodynamic notions of energy, work and dissipation must be established for these open chemical systems. Here, we do so by building upon recent theoretical advances in nonequilibrium statistical physics. As a central outcome, we show how to quantify the efficiency of such chemical operations and lay the foundation for performance analysis of any dissipative chemical process.

¹Complex Systems and Statistical Mechanics, Physics and Materials Science Research Unit, University of Luxembourg, L-1511 Luxembourg, Luxembourg.

²Present address: The Simons Center for Systems Biology, School of Natural Sciences, Institute for Advanced Study, Princeton, NJ 08540, USA.

Correspondence and requests for materials should be addressed to M.E. (email: massimiliano.esposito@uni.lu)

Traditional chemical thermodynamics deals with closed systems, which always evolve towards equilibrium. At equilibrium, all reaction currents—defined as the forward reaction fluxes minus the backwards ($J_\rho = J_{+\rho} - J_{-\rho}$, where ρ labels the reactions)—eventually vanish. The first thermodynamic description of nonequilibrium chemical processes was achieved by the Brussels school founded by de Donder and perpetuated by Prigogine^{1,2}, but they focused on few reactions close to equilibrium in the so-called linear regime. However, processes such as fuel-driven self-assembly involve open chemical reaction networks (CRN) with many reactions operating far away from equilibrium^{3,4}. The openness arises from the presence of one or more chemostats, i.e. particle reservoirs coupled with the system which externally control the concentrations of some species—just like thermostats control temperatures—and allow for matter exchanges. Open CRN can then be thought of as thermodynamic machines powered by chemostats. Two operating regimes may be distinguished, reminiscent of stroke and steady-state engines. In the first, work is used to induce a time-dependent change in the species abundances that could never be reached at equilibrium. An example could be the accumulation of a large amount of molecules with a high free energy content as in fuel-driven self-assembly, or the depletion of some undesired species as in metabolite repair⁵. In the second, work is used to maintain the system in a nonequilibrium stationary state which continuously transduces an input work into useful output work. Beyond energy transduction within pseudo-first order reactions⁶, no framework currently exists to assess how efficient and powerful such chemical engines can be. We provide one grounded in the recently established nonequilibrium thermodynamics of CRN^{7,8}, which was born from the combination of state-of-the-art statistical mechanics^{9–14} and mathematical CRN theory^{15,16}. Establishing rigorous concepts of free energy, chemical work and dissipation valid far from equilibrium reveals crucial. They provide the basis for thermodynamically meaningful definitions of efficiencies and optimal performance in the different operating regimes. In the following, energy storage (ES) and driven synthesis (DS) are analyzed as models epitomizing the first and the second operating regime, respectively, but our findings apply to any dissipative chemical process.

Results

Energy storage. In energy storage, an open CRN initially at equilibrium with high concentrations of low-energy molecules and low concentrations of high-energy ones is brought out of equilibrium with the aim to increase the concentrations of the high-energy species. This process is reminiscent of charging a capacitor via the coupling to a voltage generator. In the context of supramolecular chemistry, the concept of ES was proposed by Ragazzon and Prins⁴. An insightful model capturing its main features is described in Fig. 1. Its thermodynamic analysis, detailed in Supplementary Note 1b, will now be outlined. Given a set of reaction rate constants, the accumulation of the high-energy species A_2 may be enabled when chemostats set a certain positive chemical potential difference of fuel and waste, i.e. $\mathcal{F}_{\text{fuel}} = \mu_F - \mu_W > 0$, by steering [F] (see Supplementary Fig. 1). This implies the injection of F molecules at a rate I_F and the extraction of W at rate I_W . The resulting power (i.e., work per unit of time) performed on the system by the fueling mechanism is $\dot{W}_{\text{fuel}} = I_F \mathcal{F}_{\text{fuel}}$ ^{7,8,17}. The proper way to quantify the energy content of an open CRN is via its nonequilibrium free energy \mathcal{G} . During the charging process, only part of the work, namely $\Delta\mathcal{G}$, is dedicated to shift the concentrations distribution and is stored as free energy in the system⁴. The remaining fraction, namely $T\Sigma$, is dissipated according to the

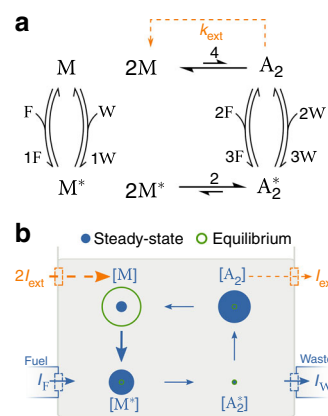


Fig. 1 Model for energy storage and driven synthesis. Without (resp. with) the orange dashed transition, the chemical reaction network models energy storage (resp. driven synthesis). The high-energy species A_2 is at low concentration at equilibrium. Powering the system by chemostating fuel (F) and waste (W) species boosts the formation of A_2 out of the monomer M via the activated species M_2 and A_2^* . **a** The chemical reaction network (forward fluxes are defined counter-clockwise). **b** Sketch of concentrations distributions (proportional to radii) and net currents (proportional to arrows thickness, see Supplementary Note 1c)

second law of thermodynamics

$$\mathcal{W}_{\text{fuel}} = \Delta\mathcal{G} + T\Sigma, \quad (1)$$

where T is temperature and $\Sigma \geq 0$ the entropy production, which only vanishes at equilibrium. The time-dependent thermodynamic efficiency of an ES process is thus the ratio

$$\eta_{\text{es}} = \frac{\Delta\mathcal{G}}{\mathcal{W}_{\text{fuel}}} = 1 - \frac{T\Sigma}{\mathcal{W}_{\text{fuel}}}. \quad (2)$$

Equation (1) has been used to derive the second equality. We emphasize that each of these contributions has an explicit expression in terms of concentrations and rate constants (see Supplementary Note 1b). For instance, the energy stored at any time with respect to equilibrium is given by the expression

$$\Delta\mathcal{G} = RT \sum_{X=M, M^*, A_2, A_2^*} \left[[X] \ln \frac{[X]}{[X]_{\text{eq}}} - [X] + [X]_{\text{eq}} \right] \geq 0, \quad (3)$$

which is reminiscent of an information theoretical measure called relative entropy¹⁸. Crucially, any concentration distribution different from the equilibrium one has a positive energy content. Equation (1) thus implies that an amount of work of at least $\Delta\mathcal{G}$ needs to be provided to reach it. It also ensures that η_{es} is bounded between zero and one.

We simulated an ES process and plotted the dynamics of concentrations as well as efficiency and its contributions in Fig. 2. The process can be divided into a charging and a maintenance phase. During the former, the system energy grows ($d_t \mathcal{G} > 0$) in a way which correlates with the accumulation of the high-energy species A_2 . The process can be quite efficient as a significant portion of the work is converted into free energy. However, in the maintenance phase, the system has reached a nonequilibrium steady state. The efficiency drops towards zero (proportional to the inverse time) as the entire work is being spent to preserve the energy previously accumulated ($d_t \mathcal{G} \simeq 0$). The maximum η_{es} is reached during the charging phase (see Supplementary Note 1b for a rigorous proof) and defines

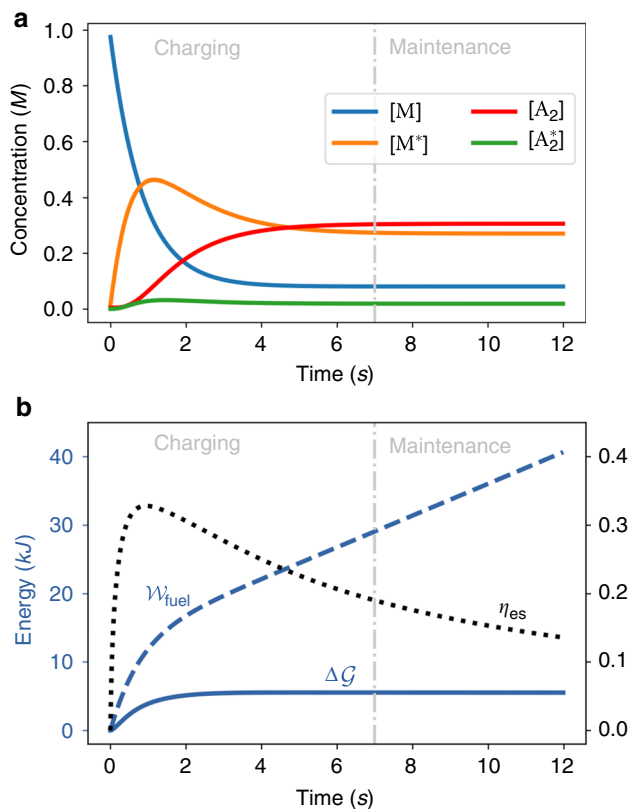


Fig. 2 Dynamics of energy storage. The system is initially prepared at thermodynamic equilibrium where $[M]_{eq} \gg [A_2]_{eq}$. At time $t = 0$, the chemical potential difference between fuel and waste is turned on at $\mathcal{F}_{fuel} = 7.5 \cdot RT$ and drives the system away from equilibrium. After a transient (charging phase), the system eventually settles into a nonequilibrium steady state (maintenance phase). **a** Species abundances. **b** Energy stored, work and efficiency (right axis, adimensional units). Kinetic constants ($\{k_{sp}\}$) and chemical potentials used for simulations are given in Supplementary Table 1

the time that minimizes the dissipation of ES. The value of the efficiency when the process enters the maintenance phase characterizes instead the performance of the ES process when the system has reached its maximum storage capacity. The best time to stop ES and start making use of it (cf. driven synthesis below) will be a tradeoff between maximizing the energy stored and minimizing dissipation. In general, the ideal situation will be the one in which η_{es} peaks as close as possible to the maintenance phase.

Figure 3 focuses on the maintenance phase for different values of \mathcal{F}_{fuel} . It shows that by driving the system away from equilibrium, one can reach species abundances that are very different with respect to the equilibrium ones. It also shows that the accumulation of free energy does not necessarily coincide with an increase in concentration of the most energetic species A_2 . Indeed, while at low values of \mathcal{F}_{fuel} the accumulation of \mathcal{G} correlates with $[A_2]$, beyond a threshold A_2 starts to be depleted while energy continues getting stored by further moving away the concentration distribution from equilibrium. We finally note that the connection of our work to “kinetic asymmetry”^{4,19} is discussed in Supplementary Note 1c.

As we have seen, the crucial part of energy storage is the charging phase, as the maintenance phase is purely dissipative and consumes chemical work without any energy gain. In order to make use of the energy accumulated during the charging phase, a mechanism extracting the energetic species from the system

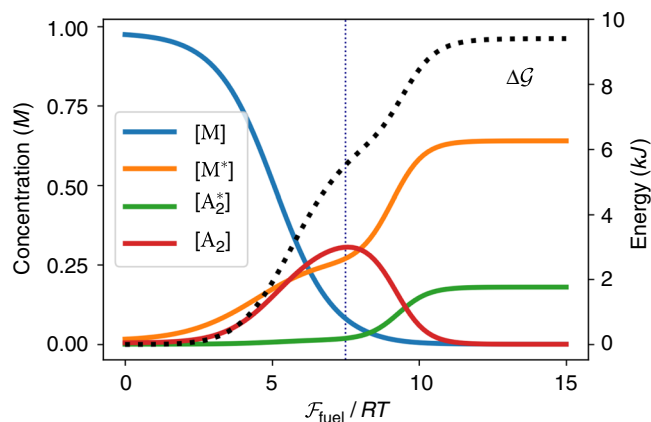


Fig. 3 Maintenance phase of energy storage. Stationary concentrations and free energy difference from equilibrium in the maintenance phase of energy storage as a function of the chemical potential difference between fuel and waste. The vertical dotted line denotes the value $\mathcal{F}_{fuel} = 7.5 \cdot RT$ used to study the charging phase in Fig. 2

must be introduced. This complementary but distinct working regime of an open CRN will now be considered.

Driven synthesis. In driven synthesis, an energetic species that accumulates thanks to a fueling process is continuously extracted from a system in a nonequilibrium steady state. One may consider for instance processes where the product either evaporates, precipitates or undergoes other fast transformations while being rapidly replaced by reactants. By building upon the above ES scheme, a simple way to model DS is to add an ideal extraction/injection mechanism to the CRN (orange dashed arrows in Fig. 1). This mechanism removes the assembled molecule A_2 and renews two M molecules at a rate $I_{ext} = k_{ext}[A_2]$. In doing so, we model the endergonic synthesis of molecules that are strongly unfavored at equilibrium, a strategy used by Nature^{20–22} and which may be within reach of supramolecular chemists^{23–25}.

From the thermodynamic standpoint detailed in Supplementary Note 2b, the input power spent by the fueling mechanism, $\dot{W}_{fuel} = I_F \mathcal{F}_{fuel} = I_F(\mu_F - \mu_W)$, is now not just dissipated as $T\dot{\Sigma}$, but part of it is used to sustain the production of A_2 :

$$\dot{W}_{fuel} = -\dot{W}_{ext} + T\dot{\Sigma}. \quad (4)$$

The output power released by the extraction mechanism, $\dot{W}_{ext} = I_{ext}(2\mu_M - \mu_{A_2})$, is negative when DS occurs. In this context the thermodynamic efficiency is thus given by

$$\eta_{ds} = -\frac{\dot{W}_{ext}}{\dot{W}_{fuel}} = 1 - \frac{T\dot{\Sigma}}{\dot{W}_{fuel}}, \quad (5)$$

where Eq. (4) has been used to derive the second equality. It is bounded between zero and one when DS occurs.

In Fig. 4, we simulated DS for various working conditions by varying k_{ext} and \mathcal{F}_{fuel} . We start our analysis by considering a given value of \mathcal{F}_{fuel} . As k_{ext} is increased, η_{ds} first grows to an optimal value before decreasing towards negative values where the DS regime ends (see Fig. 4a). At the same time I_{ext} increases until it reaches a plateau (see Fig. 4c). This happens when k_{ext} overcomes the ability of the system to sustain high values of $[A_2]$ (Fig. 4b). Eventually the drop in $[A_2]$ is such that $2\mu_M - \mu_{A_2} > 0$, thus resulting in the loss of the DS regime. We now fix k_{ext} and increase \mathcal{F}_{fuel} . The DS regime starts at a threshold value, when $[A_2]$ becomes high enough. After that, both $[A_2]$ and the efficiency grow to an optimal value before decreasing again. This time however, the efficiency remains positive as $[M]$ drops

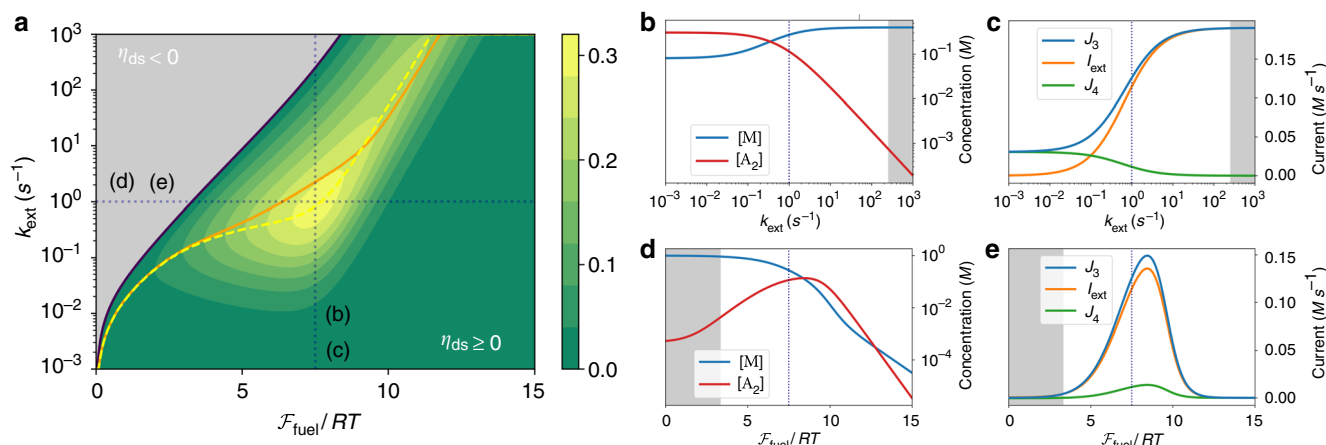


Fig. 4 Performance of driven synthesis. **a** Efficiency (η_{ds}) of driven synthesis as function of \mathcal{F}_{fuel} and k_{ext} . Regions of operating regimes that do not perform driven synthesis are colored in gray. The yellow dashed (resp. orange solid) line denotes the maximum of η_{ds} (resp. $-\dot{W}_{ext}$, see also Supplementary Fig. 2) versus k_{ext} , while the black solid line corresponds to $\eta_{ds} = 0$. **b, c** (resp. **d, e**) Concentrations and currents as a function of k_{ext} (resp. \mathcal{F}_{fuel}) along the line $\mathcal{F}_{fuel} = 7.5 \cdot RT$ (resp. $k_{ext} = 1 \text{ s}^{-1}$) highlighted by blue vertical (resp. horizontal) dotted line in plot (**a**). Kinetic constants and standard chemical potentials are the same as for ES analysis (see Supplementary Information). Note that $J_3 = I_{ext} + J_4$ always holds, where $J_3 = J_{3F} + J_{3V}$ is the net current flowing from A_2^* to A_2 .

together with $[A_2]$ (see Fig. 4d). Figure 4e shows another important feature. As \mathcal{F}_{fuel} is increased, I_{ext} first increases too, but eventually reaches a maximum after which it decreases. This phenomenon is a hallmark of far-from-equilibrium physics which could not happen in a linear regime, namely when k_{ext} and \mathcal{F}_{fuel} are small. Remarkably, the global maximum of the efficiency in Fig. 4a is reached in a region far from equilibrium. We note that it corresponds to values of \mathcal{F}_{fuel} close to the one maximizing $[A_2]$ in the maintenance phase of ES (see Fig. 3) and to values of k_{ext} of order one resulting in I_{ext} which do not overly deplete $[A_2]$. We finally turn to the lines of maximum efficiency and efficiency at maximum power in Fig. 4a, where the maximization is done with respect to k_{ext} at a given \mathcal{F}_{fuel} . Since these two lines typically do not coincide, the study of the tradeoffs is the object of a rich field called finite-time thermodynamics²⁶. Interestingly, while these two lines cannot coincide in the linear regime (see Supplementary Note 2d), we see that they do intersect far-from-equilibrium, not far from the global maximum of the efficiency. Our analysis thus allowed us to identify a region of good tradeoff between power and efficiency for the model of DS we introduced. In order to emphasize the fact that all the interesting features that we identified in DS occur far-from-equilibrium, we analyze in detail in Supplementary Note 2d the linear regime of DS. After identifying the Onsager matrix, we are able to analytically reproduce the results of the simulations in the limit of small \mathcal{F}_{fuel} and k_{ext} (bottom-left part of Fig. 4a, see Supplementary Fig. 3 for details), thus pinpointing the limit of validity of the linear regime approximation.

Discussion

Thermodynamics was born from the effort to systematize the performance of steam engines. Open CRN, which are at the core of recent efforts in artificial synthesis²⁷ and ubiquitous in living systems^{22,28,29}, can be seen as chemical engines. In the spirit of this analogy, in this article we built a chemical thermodynamic framework which enables us to systematically analyze the performance of two fundamental dissipative chemical processes. The first, energy storage, is concerned with the time-dependent accumulation of high-energy species far from equilibrium and is currently raising significant attention from supramolecular chemists. The second, driven synthesis, aims at continuously extracting the

previously obtained high-energy species and provides a simple and insightful instance of energy transduction beyond pseudo-unimolecular CRN. In doing so, we identified their optimal regimes of operation. Crucially they lie far-from-equilibrium in regions unreachable using conventional linear regime thermodynamics. We emphasize that the methods developed in this paper can in principle be applied to any open CRN and thus provide the basis for future performance studies and optimal design of dissipative chemistry. They are thus destined to play a major role in bioengineering and nanotechnologies.

Data availability

All data needed to reproduce numerical results are reported in the Supplementary Information.

Code availability

The code that generated the plots is available from the corresponding author upon request.

Received: 18 March 2019 Accepted: 18 July 2019

Published online: 27 August 2019

References

- Prigogine, I. & Defay, R. *Chemical Thermodynamics* (Longmans, Green & Co., London, 1954).
- Prigogine, I. *Introduction to Thermodynamics of Irreversible Processes* (John Wiley & Sons, New York, 1967).
- van Rossum, S. A. P., Tena-Solsona, M., van Esch, J. H., Eelkema, R. & Boekhoven, J. Dissipative out-of-equilibrium assembly of man-made supramolecular materials. *Chem. Soc. Rev.* **46**, 5519–5535 (2017).
- Ragazzon, G. & Prins, L. J. Energy consumption in chemical fuel-driven self-assembly. *Nat. Nanotechnol.* **13**, 882–889 (2018).
- Linster, C. L., Schaftingen, E. Van & Hanson, A. D. Metabolite damage and its repair or pre-emption. *Nat. Chem. Biol.* **9**, 72–80 (2013).
- Hill, T. L. *Free Energy Transduction in Biology* (Academic Press, New York, 1977).
- Rao, R. & Esposito, M. Nonequilibrium thermodynamics of chemical reaction networks: wisdom from stochastic thermodynamics. *Phys. Rev. X* **6**, 041064 (2016).
- Falasco, G., Rao, R. & Esposito, M. Information thermodynamics of turing patterns. *Phys. Rev. Lett.* **121**, 108301 (2018).
- Seifert, U. Stochastic thermodynamics, fluctuation theorems and molecular machines. *Rep. Prog. Phys.* **75**, 126001 (2012).

10. Ciliberto, S. Experiments in stochastic thermodynamics: short history and perspectives. *Phys. Rev. X* **7**, 021051 (2017).
11. Jarzynski, C. Equalities and inequalities: irreversibility and the second law of thermodynamics at the nanoscale. *Annu. Rev. Condens. Matter Phys.* **2**, 329–351 (2011).
12. Zhang, X.-J., Qian, H. & Qian, M. Stochastic theory of nonequilibrium steady states and its applications. Part i. *Phys. Rep.* **510**, 1–86 (2012).
13. Ge, H., Qian, M. & Qian, H. Stochastic theory of nonequilibrium steady states and its applications. Part ii: applications in chemical biophysics. *Phys. Rep.* **510**, 87–118 (2012).
14. Van den Broeck, C. & Esposito, M. Ensemble and trajectory thermodynamics: a brief introduction. *Phys. A* **418**, 6–16 (2015).
15. Horn, F. & Jackson, R. General mass action kinetics. *Arch. Ration. Mech. An.* **47**, 81–116 (1972).
16. Feinberg, M. Complex balancing in general kinetic systems. *Arch. Ration. Mech. An.* **49**, 187–194 (1972).
17. Rao, R. & Esposito, M. Conservation laws and work fluctuation relations in chemical reaction networks. *J. Chem. Phys.* **149**, 245101 (2018).
18. Cover, T. M. & Thomas, J. A. *Elements of Information Theory* (John Wiley & Sons, New York, 2006).
19. Astumian, R. D. Stochastic pumping of non-equilibrium steady-states: how molecules adapt to a fluctuating environment. *ChemComm.* **54**, 427–444 (2018).
20. Desai, A. & Mitchison, T. J. Microtubule polymerization dynamics. *Annu. Rev. Cell. Dev. Biol.* **13**, 83–117 (1997).
21. Howard, J. *Mechanics of Motor Proteins and the Cytoskeleton* (Sinauer Associates, Sunderland, MA, 2001).
22. Hess, H. & Ross, J. L. Non-equilibrium assembly of microtubules: from molecules to autonomous chemical robots. *Chem. Soc. Rev.* **46**, 5570–5587 (2017).
23. Boekhoven, J. et al. Dissipative self-assembly of a molecular gelator by using a chemical fuel. *Angew. Chem.* **122**, 4935–4938 (2010).
24. Boekhoven, J., Hendriksen, W. E., Koper, G. J. M., Elkema, R. & van Esch, J. H. Transient assembly of active materials fueled by a chemical reaction. *Science* **349**, 1075–1079 (2015).
25. Sorrenti, A., Leira-Iglesias, J., Markvoort, A. J., de Greef, T. F. A. & Hermans, T. M. Non-equilibrium supramolecular polymerization. *Chem. Soc. Rev.* **46**, 5476–5490 (2017).
26. Benenti, G., Casati, G., Saito, K. & Whitney, R. S. Fundamental aspects of steady-state conversion of heat to work at the nanoscale. *Phys. Rep.* **694**, 1–124 (2017).
27. Mattia, E. & Otto, S. Supramolecular systems chemistry. *Nat. Nanotechnol.* **10**, 111 (2015).
28. Zwaag, Dvander & Meijer, E. W. Fueling connections between chemistry and biology. *Science* **349**, 1056–1057 (2015).
29. Grzybowski, B. A. & Huck, W. T. S. The nanotechnology of life-inspired systems. *Nat. Nanotechnol.* **11**, 585 (2016).

Acknowledgements

This work was funded by the Luxembourg National Research Fund (AFR Ph.D. Grant 2014-2, No. 9114110) and the European Research Council project NanoThermo (ERC-2015-CoG Agreement No. 681456).

Author contributions

E.P., R.R., and M.E. all significantly contributed to conceive and realize the project as well as in writing the paper.

Additional information

Supplementary Information accompanies this paper at <https://doi.org/10.1038/s41467-019-11676-x>.

Competing interests: The authors declare no competing interests.

Reprints and permission information is available online at <http://npj.nature.com/reprintsandpermissions/>

Peer review information: *Nature Communications* thanks the anonymous reviewers for their contribution to the peer review of this work. Peer reviewer reports are available.

Publisher's note: Springer Nature remains neutral with regard to jurisdictional claims in published maps and institutional affiliations.



Open Access This article is licensed under a Creative Commons Attribution 4.0 International License, which permits use, sharing, adaptation, distribution and reproduction in any medium or format, as long as you give appropriate credit to the original author(s) and the source, provide a link to the Creative Commons license, and indicate if changes were made. The images or other third party material in this article are included in the article's Creative Commons license, unless indicated otherwise in a credit line to the material. If material is not included in the article's Creative Commons license and your intended use is not permitted by statutory regulation or exceeds the permitted use, you will need to obtain permission directly from the copyright holder. To view a copy of this license, visit <http://creativecommons.org/licenses/by/4.0/>.

© The Author(s) 2019